42.85-hour imposed day length. The ratio of scheduled bedtime to scheduled wake time was maintained at 1:2 for each forced desynchrony protocol.

31. Using the NOSA technique, core-temperature data collected throughout the month-long experiment were modeled as a harmonic regression model with continuous first-order autoregressive [AR(1)] noise defined as

$$y_t = s_t + x_t + v_t \quad (1)$$

where y_t is the core-temperature measurement at time t, s_t is the circadian signal, x_t is the forced desynchrony component, and v_t is the AR(1) noise. We define

$$s_t = \mu + \sum_{r=1}^{2} A_r \cos\left(\frac{2\pi rt}{\tau}\right) + B_r \sin\left(\frac{2\pi rt}{\tau}\right) \quad (2a)$$

$$x_t = \sum_{k=1}^{8} C_k \cos\left(\frac{2\pi kt}{28}\right) + D_k \sin\left(\frac{2\pi kt}{28}\right) \quad (2b)$$

$$v_t = \exp(-\alpha\Delta)v_{t-1} + \varepsilon_t \quad (2c)$$

where μ is mean temperature, τ is the intrinsic period of the circadian pacemaker, A_r and B_r are respectively the cosine and sine coefficients of the r^{th} harmonic of the circadian signal, C_k and D_k are respectively the cosine and sine coefficients of the k^{th} harmonic of the forced desynchrony component, Δ is the sampling interval, α is the approximate time constant of the thermoregulatory system, and the ε_t's are independent, identically distributed Gaussian noise with zero mean and variance σ_ε^2. The variance of v_t is $\sigma_v^2 = \sigma_\varepsilon^2[1 - \exp(-2\alpha\Delta)]^{-1}$. The choice of two harmonics to model the circadian component is based on Brown and Czeisler (*32*), whereas the choice of eight harmonics to model the forced desynchrony component was determined empirically. The model was fit to the data by an exact maximum likelihood method [R. H. Jones, *Longitudinal Data with Serial Correlation: A State-Space Approach* (Chapman & Hall, New York, 1993); E. N. Brown and C. H. Schmid, in *Methods in Enzymology, Numerical Computer Methods, Part B*, L. Brand and M. L. Johnson, Eds. (Academic Press, Orlando, FL, 1994), pp. 171–181]. The standard deviation of the period estimate used to compute the 95% confidence intervals for τ was computed as

$$\sigma_\tau = \left\{ \frac{6\tau^4 \sigma_\varepsilon^2 \Delta[1 - \exp(-2\alpha\Delta)]}{\pi^2 T^3 \sum_{r=1}^{2} r^2(A_r^2 + B_r^2)\left[1 - 2\exp(-\alpha\Delta)\cos\left(\frac{2\pi r\Delta}{\tau}\right) + \exp(-2\alpha\Delta)\right]} \right\}^{\frac{1}{2}} \quad (3)$$

where T is the study length [E. N. Brown, V. Solo, Y. Choe, Z. Zhang, *Tech. Rep. 95-01* (Statistics Research Laboratory, Department of Anesthesia and Critical Care, Massachusetts General Hospital, April 1996; revised November 1997)]. The hormone measurements have no thermoregulatory component; hence, for their analyses, we used the model in Eq. 2 with $v_t = \varepsilon_t$, and the formula in Eq. 3 with $\alpha = \infty$. For the free-running studies, only core body temperature was sampled and the fitting did not include a forced period. NOSA can include periodic terms that may arise from nonlinear interactions between the basic periodic signals s_t and x_t. We have explored such additional terms and identified those that rise above the level of noise in the temperature data. However, when these are included, the effect on the average endogenous period reported here is minimal (<1 min) and not statistically significant. We therefore report the endogenous periods estimated without interaction periodicities, which can be used to investigate related nonlinear processes that are beyond the scope of this report.

32. E. N. Brown and C. A. Czeisler, *J. Biol. Rhythms* **7**, 177 (1992).
33. T. L. Shanahan and C. A. Czeisler, *Sleep Res.* **20A**, 557 (1991); T. L. Shanahan, thesis, Harvard Medical School (1995).
34. J. K. Wyatt *et al.*, *Sleep Res.* **26**, 759 (1997); D. W. Rimmer, D. J. Dijk, J. K. Wyatt, D. F. Dinges, C. A. Czeisler, *Med. Sci. Sports Exercise* **30**, 5 (1997).
35. Free-running subjects, who self-selected the timing of their sleep-wake and light-dark schedule while living in an environment free of time cues, chose sleep episode fractions averaging 29 to 33% (*8, 12, 13, 36, 37, 39*), comparable to the sleep fraction imposed in the forced desynchrony reported herein.
36. C. A. Czeisler, E. D. Weitzman, M. C. Moore-Ede, J. C. Zimmerman, R. S. Knauer, *Science* **210**, 1264 (1980).
37. J. Zulley, R. Wever, J. Aschoff, *Pfluegers Arch.* **391**, 314 (1981).
38. This same mechanism by which free-running subjects exhibit a longer observed period than their actual intrinsic circadian period may underlie some clinical cases of non–24-hour sleep-wake schedule disorder in which subjects exhibit an average sleep-wake cycle duration of ≥25 hours, even though their actual intrinsic circadian period may be much closer to 24 hours [J. S. Emens, D. J. Brotman, C. A. Czeisler, *Sleep Res.* **23**, 256 (1994)]. Thus, their disorder may be behaviorally self-induced via self-selected exposure to artificial light, rather than being the result of an aberrant intrinsic circadian period.
39. C. A. Czeisler, thesis, Stanford University (1978).
40. L. P. Morin, K. M. Fitzgerald, I. Zucker, *Science* **196**, 305 (1977); K.-I. Honma, S. Honma, T. Hiroshige, *Jpn. J. Physiol.* **35**, 643 (1985); D. M. Edgar and W. C. Dement, *Am. J. Physiol.* **261**, R928 (1991); P. J. Shiromani and D. Overstreet, *Biol. Psychiatry* **36**, 622 (1994); R. E. Kronauer, C. A. Czeisler, S. F. Pilato, M. C. Moore-Ede, *Am. J. Physiol.* **242**, R3 (1982); A. Gundel and M. B. Spencer, *Chronobiol. Int.* **9**, 148 (1992).
41. A. E. Hiddinga, D. G. M. Beersma, R. H. van den Hoofdakker, *J. Sleep Res.* **6**, 156 (1997).
42. J. Zulley and S. S. Campbell, *Hum. Neurobiol.* **4**, 123 (1985); N. Mrosovsky, *Nature* **319**, 536 (1986).
43. We reanalyzed the body temperature data recorded during the first week of our 28-hour forced desynchrony protocol (1 beat cycle) and the first 5 days of the 20-hour forced desynchrony protocol [also 1 beat cycle and identical to the duration of the experiment in (*41*)]. Estimation of circadian period on this shortened data series increased the variance of our period estimate by a factor of more than 13 in the case of the 28-hour protocol and by a factor of more than 6 in the case of the 20-hour protocol, as would be predicted by our statistical model, in which the variance of the period estimate decreases as $1/T^3$ (*31*).
44. D. Minors *et al.*, *Chronobiol. Int.* **13**, 179 (1996).
45. T. L. Kelly *et al.*, *J. Biol. Rhythms* **14**, 190 (1999).
46. R. L. Sack, A. J. Lewy, M. L. Blood, L. D. Keith, H. Nakagawa, *J. Clin. Endocrinol. Metab.* **75**, 127 (1992); D. N. Orth, G. M. Besser, P. H. King, W. E. Nicholson, *Clin. Endocrinol.* **10**, 603 (1979); S. W. Lockley *et al.*, *J. Clin. Endocrinol. Metab.* **82**, 3763 (1997).
47. A. Eskin, in *Biochronometry*, M. Menaker, Ed. (National Academy of Sciences, Washington, DC, 1971), pp. 55–80.
48. F. C. Davis and N. Viswanathan, *Am. J. Physiol.* **275**, R960 (1998); J. F. Duffy, thesis, Northeastern University (1998).
49. M. A. Carskadon, S. E. Labyak, C. Acebo, R. Seifer, *Neurosci. Lett.* **260**, 129 (1999).

50. We thank the subject volunteers; research technicians; senior research technicians A. Fergus, K. Foote, G. Jayne, E. Martin, and A. Ward; S. Driscoll and the staff of the General Clinical Research Center (GCRC) of Brigham and Women's Hospital; subject recruiters J. Daley, J. Kao, D. Margolis, and R. McCarley; research assistants D. Chen and J. Whittemore Jr.; the Clinical Core Laboratory of the GCRC and Elias USA Inc. for hormonal assays; T. Ding for analytic software; W. Freitag for management of bioengineering systems; L. Rosenthal for illustrations; J. Zeitzer for comments; J. K. Wyatt for provision of comparative data; and G. H. Williams for overall support. Supported by the U.S. Public Health Service National Institute on Aging Award PO1-AG09975 (C.A.C.), National Institute of General Medical Sciences Award R01-GM53559 (E.N.B.), and NASA Cooperative Agreement NCC9-58 with the National Space Biomedical Research Institute. The studies were performed in a GCRC supported by MO1-RR02635. This paper is dedicated to the memory of Professor Jürgen Aschoff (1913–1998), who pioneered the modern science of circadian biology and established the first continuously operational laboratory shielded from external time cues to study human circadian physiology.

7 October 1998; accepted 17 May 1999

Arabidopsis Galactolipid Biosynthesis and Lipid Trafficking Mediated by DGD1

Peter Dörmann,[1] Ilse Balbo,[2] Christoph Benning[1]*

The photosynthetic apparatus in plant cells is associated with membranes of the thylakoids within the chloroplast and is embedded into a highly specialized lipid matrix. Diacylglycerol galactolipids are common in thylakoid membranes but are excluded from all others. Isolation of the gene *DGD1*, encoding a galactosyltransferase-like protein, now provides insights into assembly of the thylakoid lipid matrix and subcellular lipid trafficking in *Arabidopsis thaliana*.

Of the four lipids associated with thylakoid membranes in plants only one is a phospholipid, the ubiquitous phosphatidylglycerol. The other three are nonphosphorous diacylglycerol glycolipids with one or two galactose moieties or a sulfonic acid derivative of glucose attached to diacylglycerol (*1*). The galactolipids constitute the bulk (close to 80%) of the thylakoid lipid matrix and, within green plant parts, 70 to 80% of the lipids are associated with photosynthetic membranes. Most vegetables and fruits in human and animal diets are rich in galactolipids. Their breakdown products represent an important dietary source of galactose and polyunsaturated fatty acids (*2*).

Thylakoid membrane lipid biosynthesis in plants requires both carbohydrate and fatty acid metabolic pathways and is not restricted to chloroplasts, where galactolipids are found

[1]Department of Biochemistry, Michigan State University, East Lansing, MI 48824, USA. [2]Max-Planck-Institut für Molekulare Pflanzenphysiologie, D-14476, Golm, Germany.

*To whom correspondence should be addressed. E-mail: benning@pilot.msu.edu

(Fig. 1); it also involves enzymes in the endoplasmic reticulum (ER). Subcellular trafficking is required to transfer lipid moieties from the ER to their ultimate destination in the thylakoid. Molecular species of galactolipids can be distinguished on the basis of their fatty acid constituents (*3*). Lipid moieties assembled inside the chloroplast tend to include a 16-carbon fatty acid in the *sn*2 position of diacylglycerol, whereas lipids derived from the ER pathway tend to contain an 18-carbon fatty acid in this position because acyltransferases of the plastid and the ER have different substrate specificities. The plastid pathway is dispensable in many plants (*4*), but no naturally occurring plant without a functional ER pathway is known. One mutant of *Arabidopsis*, *act1* (acyltransferase 1), is deficient in the plastid acyltransferase (*5*) that catalyzes lysophosphatidic acid biosynthesis (Fig. 1). Other *Arabidopsis* mutants with an altered lipid composition (*6*) are deficient in fatty acid desaturases.

The *dgd1* (digalactosyldiacylglycerol 1) mutant of *Arabidopsis* (*7*) is impaired in galactolipid assembly as suggested by a 90% reduction in digalactosyl lipid content (Table 1). Growth, chloroplast ultrastructure, composition and ratios of different pigment protein complexes, light utilization, and chloroplast protein import are affected in *dgd1* (*8*). The *dgd1* mutant also shows an altered composition of the monogalactosyl lipid with a characteristic increase in molecular species containing 18-carbon fatty acids (Table 1), consistent with their presumed precursor function in digalactosyl lipid biosynthesis (see below).

Based on labeling experiments with isolated chloroplasts, it has been proposed (*9*) that one galactose moiety is transferred from one monogalactosyl lipid onto a second to form the digalactosyl lipid (Fig. 1). The released diacylglycerol moiety is made available for further thylakoid lipid assembly, with the bulk appearing in the monogalactosyl lipid. As can be assumed from the fatty acid composition of the digalactosyl lipid in the wild type (*10*) (Table 1), the responsible enzyme is specific for molecular species derived from the ER. Accordingly, approximately equal amounts of ER-derived molecular species are found in the digalactosyl and monogalactosyl lipids in the wild type (Fig.1). Therefore, disruption of digalactosyl lipid biosynthesis in the *dgd1* mutant would disturb assembly of other thylakoid lipids, in particular the ER-derived monogalactosyl lipid.

To test this hypothesis, we constructed an *act1,dgd1* double mutant (*11*) (Fig. 1). The double mutant (Fig. 2) showed a more extremely stunted phenotype than either parent. Because the lipid composition of the double mutant was not too unlike that of either parent (Table 1), it is improbable that the extreme growth phenotype of the double mutant is due to specific lipid effects. However, the double mutant may not be able to produce sufficient amounts of thylakoid membranes, because both plastid and ER pathways are disrupted (Fig. 1).

At least two genes encoding putative monogalactosyl lipid synthases are present in *Arabidopsis* (GenBank accession numbers AJ000331 and AL031004), which may have different substrate specificities and different associations with the chloroplast inner or outer envelope (*12–15*). According to the model (Fig. 1), a transient pool of monogalactosyl lipid is produced at the outer envelope from ER-derived diacylglycerol and is immediately converted by DGD1. This process is accompanied by a transfer of lipid moieties from the outer to the inner envelope. In the absence of DGD1, monogalactosyl lipid cannot be efficiently synthesized via the ER pathway but the plastid pathway can compensate for this deficiency. Only when both pathways are blocked, as in the *act1,dgd1* double mutant, is the overall galactolipid biosynthesis insufficient to support growth. Apparently, the proposed initial biosynthesis of galactolipids at the outer envelope membrane cannot compensate for biosynthesis by DGD1 but would explain the small amount of digalactosyl lipid and the altered molecular species composition of monogalactosyl lipid in *dgd1*. Processes in parallel to the DGD1 pathway may permit a less efficient transfer of lipids to the thylakoids in the *dgd1* mutant (Fig. 1) responsible for moderate growth (Fig. 2). In the *act1* mutant, which is not stunted, only the ER pathway is fully opera-

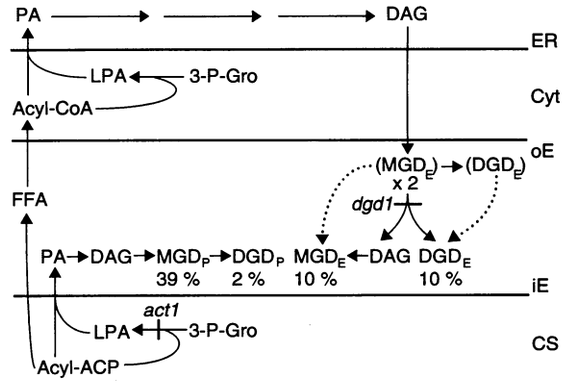

Fig. 1. Galactolipid biosynthesis in *Arabidopsis*. Diacylglycerol (DAG) derived from either the chloroplast or the ER pathway serves as a precursor for biosynthesis of monogalactosyldiacylglycerol [1,2-diacyl-3-*O*-(β-D-galactopyranosyl)-*sn*-glycerol; MGD], and MGD is a precursor of digalactosyldiacylglycerol {1,2-diacyl-3-*O*-[α-D-galactopyranosyl-(1→6)-*O*-β-D-galactopyranosyl]-*sn*-glycerol; DGD}. Subscripts P and E indicate the origin of lipids from plastid and ER pathways. The contribution of each pathway in the wild type is indicated [mol% of total polar lipids derived from positional fatty acid analysis according to (*10*)]. The proposed membrane association of the respective enzymes is indicated. Transient pools of MGD$_E$ and DGD$_E$ are shown in parentheses. Dotted arrows indicate inefficient processes bypassing the *dgd1* block. ACP, acyl carrier protein; CS, chloroplast stroma; Cyt, cytosol; iE, inner envelope membrane; oE, outer envelope membrane; FFA free fatty acids; LPA, lysophosphatidic acid; PA, phosphatidic acid; 3-P-Gro, 3-phosphoglycerol.

Table 1. Fatty acid composition of galactolipids in different lines of *Arabidopsis*. Relative amounts (mol% of total fatty acids in lipid) of 7,10,13-hexadecatrienoic acid (all-*cis*-16:3$\Delta^{7,10,13}$) and α-linolenic acid (all-*cis*-18:3$\Delta^{9,12,15}$) in the two galactolipids as well as their fraction of total polar lipids (mol%) were determined by fatty acid methyl ester quantification in leaves from plants grown in tissue culture. SDs (three experiments) were <2.5% (galactolipids) and <1.0% (fatty acids). ND, not detectable.

	Wild type	*dgd1*	*act1*	*act1,dgd1*
Monogalactosyldiacylglycerol	49.8	53.5	53.7	44.2
7,10,13-Hexadecatrienoic acid	28.9	14.1	0.8	0.7
α-Linolenic acid	62.5	78.5	88.5	86.4
Digalactosyldiacylglycerol	12.0	1.7	15.9	2.1
7,10,13-Hexadecatrienoic acid	2.6	2.8	ND	ND
α-Linolenic acid	71.1	41.2	83.0	44.6

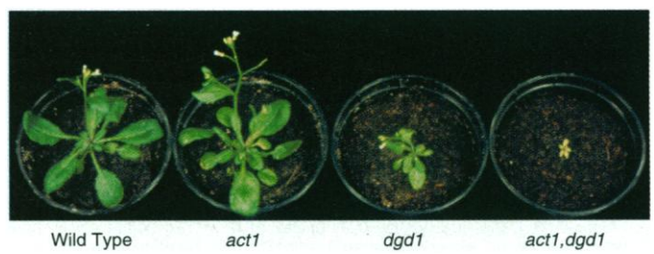

Fig. 2. Appearance of the *act1,dgd1* double mutant of *Arabidopsis*. Four-week-old plants raised in soil of the wild type (ecotype Col-2), the single homozygous mutants *act1* and *dgd1*, and the *act1,dgd1* double homozygous mutant.

tional, yet the ratio of mono- to digalactosyl lipid is not 1:1 as would be predicted by the proposed DGD1 pathway. However, secondary processes such as differential lipid turnover aimed at maintaining proper lipid composition may come into play in *act1*.

We isolated the *DGD1* locus and corresponding *DGD1* cDNA by a strategy based on the map position of *dgd1*. Resolution of the heterogeneous *dgd1* genetic background with markers characteristic for ecotypes Col-2 or L*er* interspersed close to the *dgd1* locus was achieved by integration of mapping populations derived from crosses of *dgd1* to Col-2 or L*er* wild type (*16*). The mutant phenotype was analyzed by thin-layer chromatography (TLC) of leaf lipid extracts; during fine mapping it was necessary to process several thousand samples. The map generated encompasses the *DGD1* locus and the yeast artificial chromosome (YAC), bacterial artificial chromosome (BAC), and cosmid contigs spanning the locus on chromosome 3 (Fig. 3) (*17*). Different cosmids harboring inserts between T-DNA borders were tested for complementation. Because the *dgd1* mutant could not be transformed with large genomic fragments, we transferred the cosmid inserts into the wild type and crossed the T-DNA into the *dgd1* mutant (*18*). Analysis of three F_2 populations derived from crosses with independent lines containing cosmid C49B was consistent with genetic complementation by a gene on C49B. Sequencing of portions of C49B (GenBank accession number AF149842) identified a putative gene located in the center of C49B, which was predicted to represent the *DGD1* locus. Therefore, C49B was used to screen a cDNA library (*19*). We identified and sequenced a 2649-base-pair (bp) cDNA (GenBank accession number AF149841) (Fig. 3D). This cDNA appeared to be complete because it contained in-frame stop codons 5′ of a putative start codon. The cDNA was inserted behind a cauliflower mosaic virus (CaMV) 35*S* promoter and transferred directly into the mutant by *Agrobacterium*-mediated in planta transformation (*20*). Two transgenic plants were recovered and both were phenotypically wild type with regard to growth habit and lipid composition, which indicates complementation. Genetically homozygous *dgd1* plants were identified in each complementation experiment by DNA-DNA hybridization with the restriction fragment length polymorphism (RFLP) marker 5E-5, which scores identical in Col-2 and L*er* wild-type backgrounds but different in *dgd1*. Cosmid C49B and the *DGD1* cDNA lead to wild-type lipid composition in all tested transgenic plants homozygous for *dgd1*.

To obtain independent evidence for the identity of the *DGD1* locus, we sequenced the *DGD1* and *dgd1* loci. Comparison of the genomic and cDNA sequences revealed seven exons and a transition of a CAA (glutamine) to a TAA (stop) codon in exon 6 in the *dgd1* allele. The *DGD1* cDNA is predicted to encode a 91.8-kD protein with weak sequence similarity in the COOH-terminal portion to bacterial and plant glycosyltransferases. To determine the biosynthetic activity of the *DGD1* gene product, the *DGD1* cDNA was expressed in *Escherichia coli* along with the monogalactosyl lipid synthase previously isolated from cucumbers (*12, 21*). In addition to monogalactosyl lipid, another glycolipid was observed that comigrates with an authentic digalactosyl lipid standard. In essence, we were able to reconstitute the plant galactolipid biosynthetic pathway in *E. coli* (Fig. 4). Expression of *DGD1* alone did not lead to digalactosyl lipid biosynthesis. Thus, the *DGD1* gene indeed encodes a digalactosyl lipid synthase that requires monogalactosyl lipid as substrate.

A similar gene (BLASTP score 360) located on chromosome 4 (BAC F6N23) of *Arabidopsis* (tentatively designated *DGD2*) is predicted to encode a protein missing about 340 amino acids of the NH_2-terminal portion compared with DGD1, but it shows similarity to the glycosyltransferase-like sequence part of DGD1. The predicted DGD1 protein contains an NH_2-terminal transit peptide typical for proteins imported into the plastid and two strongly hydrophobic domains (amino acids 347 to 372 and 644 to 670). This observation agrees with a proposed association of DGD1 with the plastid envelope membranes (*14, 22*). The availability of the *DGD1* gene, the similar *DGD2* gene, and genes encoding monogalactosyl lipid synthases of *Arabidopsis* will promote investigations into galactolipid biosynthesis and subcellular lipid trafficking.

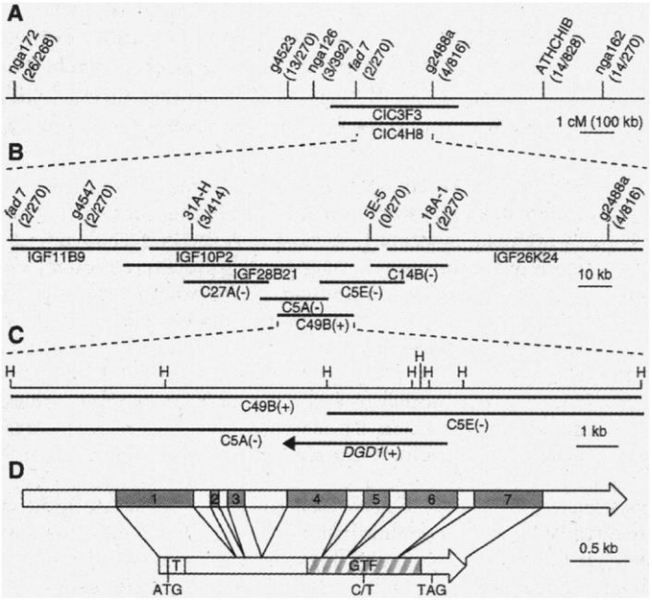

Fig. 3. Positional cloning of the *DGD1* gene. **(A)** Partial genetic map of *Arabidopsis* chromosome 3 and YAC clones containing *DGD1*. Numbers in parentheses indicate recombinations between marker and *dgd1* per number of chromosomes analyzed. **(B)** Fine mapping between markers *fad7* and g2488a as well as BAC (IGF clone no.) and cosmid (C clone no.) contigs. +, complementing clones; −, noncomplementing clones. **(C)** Map of C49B, C5A, and C5E. H, Hind III restriction sites. **(D)** Structure of *DGD1* gene and cDNA. Exons are shaded and numbered. The predicted chloroplast transit peptide (T) is indicated as well as the part showing similarity to glycosyltransferases (GTF; cross-hatched), the start (ATG) and stop (TAG) codons, and the C-to-T mutation (C/T) in the *dgd1* allele. GenBank accession numbers: genomic sequence, AF149842; cDNA, AF149841.

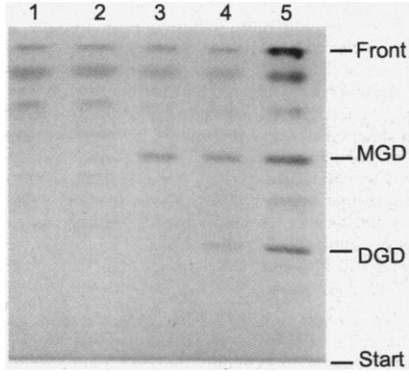

Fig. 4. Reconstitution of the plant galactolipid biosynthetic pathway in *E. coli*. The *Arabidopsis DGD1* and cucumber monogalctosyl lipid synthase cDNAs were introduced into *E. coli* on two compatible plasmids. Glycolipids were separated by TLC and visualized with α-naphthol. Lane 1, *E. coli* without plasmid; lane 2, *E. coli* containing only plasmid pACYC-31/239 (*DGD1* cDNA); lane 3, *E. coli* containing the monogalactosyl lipid synthase and empty pACYC-31 vector; lane 4, *E. coli* containing the monogalactosyl lipid synthase and pACYC-31/239 (*DGD1* cDNA); lane 5, polar lipids from *Arabidopsis* wild-type leaves.

References and Notes

1. J. Browse and C. Somerville, *Annu. Rev. Plant Physiol. Plant Mol. Biol.* **42**, 467 (1991); J. Joyard *et al.*, *Plant Physiol.* **118**, 715 (1998).
2. L. Ohlsson, M. Blom, K. Bohlinder, A. Carlsson, A. Nilsson, *J. Nutr.* **128**, 239 (1998); L. Andersson *et al.*, *J. Lipid Res.* **36**, 1392 (1995).

3. E. Heinz and P. G. Roughan, *Plant Physiol.* **72**, 273 (1983).
4. S. Mongrand, J.-J. Bessoule, F. Cabantous, C. Cassagne, *Phytochemistry* **49**, 1049 (1998).
5. L. Kunst, J. Browse, C. R. Somerville, *Proc. Natl. Acad. Sci. U.S.A.* **85**, 4143 (1988).
6. J. Browse and C. R. Somerville, in *Arabidopsis*, E. M. Meyerowitz and C. R. Somerville, Eds. (Cold Spring Harbor Laboratory Press, Cold Spring Harbor, NY, 1994), pp. 881–912.
7. P. Dörmann, S. Hoffmann-Benning, I. Balbo, C. Benning, *Plant Cell* **7**, 1801 (1995).
8. H. Härtel, H. Lokstein, P. Dörmann, B. Grimm, C. Benning, *Plant Physiol.* **115**, 1175 (1997); F. Reifarth *et al.*, *Biochemistry* **36**, 11769 (1997); H. Härtel, H. Lokstein, P. Dörmann, R. N. Trethewey, C. Benning, *Plant Physiol. Biochem.* **36**, 407 (1998); L.-J. Chen and H.-M. Li, *Plant J.* **16**, 33 (1998).
9. A. van Besouw and J. F. G. M. Wintermans, *Biochim. Biophys. Acta* **529**, 44 (1978); J. W. M. Heemskerk, T. Storz, R. R. Schmidt, E. Heinz, *Plant Physiol.* **93**, 1286 (1990).
10. J. Browse, N. Warwick, C. R. Somerville, C. R. Slack, *Biochem. J.* **235**, 25 (1986).
11. An F_2 population of plants derived from the cross of *act1* (*Arabidopsis* Biological Resource Center, Columbus, OH) and *dgd1* was screened by TLC or gas chromatography. About 1/16th of the F_2 plants were homozygous *act1*,*dgd1* double mutants with reduced amounts of 7,10,13-hexadecatrienoic acid as in *act1* and reduced amounts of the digalactosyl lipid as in *dgd1*.
12. M. Shimojima *et al.*, *Proc. Natl. Acad. Sci. U.S.A.* **94**, 333 (1997).
13. M. A. Block, A.-J. Dorne, J. Joyard, R. Douce, *J. Biol. Chem.* **258**, 13281 (1983).
14. K. Cline and K. Keegstra, *Plant Physiol.* **71**, 366 (1983).
15. T. Teucher and E. Heinz, *Planta* **184**, 319 (1991); E. Maréchal, M. A. Block, J. Joyard, R. Douce, *J. Biol. Chem.* **269**, 5788 (1994).
16. Of 135 F_2 plants derived from the cross *dgd1* × Col-2, plants with crossovers between markers nga162 and nga172 were selected [C. J. Bell and J. R. Ecker, *Genomics* **19**, 137 (1994)]. In this F_2 population, we mapped the *DGD1* locus relative to markers g4523, *fad7*, g4547, 5E-5, and 18A-1. Similarly, we screened 424 F_2 plants from the cross *dgd1* × *Ler* for crossovers between markers nga127 and ATHCHIB. We used this mapping population to score markers g2488a and 31A-H. We obtained the RFLP markers from the *Arabidopsis* Biological Resource Center (g4523, *fad7*, g2488a, g4547) or from genomic fragments (31A-H, 5E-5, 18A-1) isolated from cosmids.
17. We used DNA of *fad7*, g4547, and g2488a to isolate genomic DNA fragments from different libraries {CIC yeast artificial chromosome library [C. Camilleri *et al.*, *Plant J.* **14**, 633 (1998)], IGF bacterial artificial chromosome library [T. Mozo, S. Fischer, H. Shizuya, T. Altmann, *Mol. Gen. Genet.* **258**, 562 (1998)], and *Arabidopsis* cosmid library [K. Meyer, G. Benning, E. Grill, in *Genome Mapping in Plants*, A. H. Patterns, Ed. (Academic Press, New York, 1996), pp. 137–154]}.
18. Cosmid clones were transferred into *Agrobacterium tumefaciens* C58C1(pGV2260) and used to transform *Arabidopsis* Col-2 wild type by vacuum infiltration [N. Bechtold, J. Ellis, G. Pelletier, *C. R. Acad. Sci. Ser. III Life Sci.* **316**, 1194 (1993); A. F. Bent *et al.*, *Science* **265**, 1856 (1994)]. We crossed transformants with *dgd1* plants and analyzed segregation in the F_2 generation. Complementation was assumed when of a minimum of 100 tested F_2 plants (one to three independent crosses per cosmid) carrying the T-DNA, all were phenotypically wild type.
19. U. Uwer, L. Willmitzer, T. Altmann, *Plant Cell* **10**, 1277 (1998).
20. For direct complementation analysis, the *DGD1* cDNA released from pBluescriptIISK(+) with Sma I, Xho I was ligated into Sma I, Sal I of pBINAR-Hyg [D. Becker, *Nucleic Acids Res.* **18**, 203 (1990); A. von Schaeven, thesis, Freie Universität Berlin (1989)] in the sense orientation behind the CaMV 35S promoter. This construct was directly transferred into *dgd1*.
21. A 459-bp Xho I, Pvu II fragment including the expression cassette was isolated from pQE31 (Qiagen Inc.) and ligated into the Sal I, Eco RV sites of pACYC184 [A. C. Y. Chang and S. N. Cohen, *J. Bacteriol.* **134**, 1141 (1978)], giving rise to the plasmid pACYC-31. We amplified the open reading frame of the *DGD1* cDNA by polymerase chain reaction with the primers (5′-GCGGATCCGGTAAAGGAAACTCTAATT) and (5′-TTCTGCAGTCTACCAGCCGAAGATTGG), thereby introducing a Bam HI site at the 5′ terminus and a Pst I site at the 3′ terminus. We ligated this cDNA fragment (Bam HI/Pst I) into pACYC-31. The resulting plasmid pACYC-31/239 was transferred into XL1-Blue cells containing the expression vector pGEX-3X with the cucumber monogalactosyl lipid synthase cDNA (*12*).
22. A.-J. Dorne, M. A. Block, J. Joyard, R. Douce, *FEBS Lett.* **145**, 30 (1982).

23. Supported in part by grants from the US Department of Energy and from the Bundesministerium für Bildung und Forschung to C.B. and by a Feodor Lynen fellowship from the Alexander von Humboldt-Foundation and a research scholarship from the Deutsche Forschungsgemeinschaft to P.D. We are indebted to Ed Tolbert for stimulating discussions up until his death in December 1998. We thank H. Ohta for providing the monogalactosyl lipid synthase plasmid. We are grateful to B. Hintzmann and A. Rosenthal for sequencing genomic DNA and cDNA clones. The help of J. Huber in screening and analyzing complemented plants is especially acknowledged.

10 March 1999; accepted 19 May 1999

Receptor for Motilin Identified in the Human Gastrointestinal System

Scott D. Feighner,[1]* Carina P. Tan,[1]* Karen Kulju McKee,[1]* Oksana C. Palyha,[1] Donna L. Hreniuk,[1] Sheng-Shung Pong,[1] Christopher P. Austin,[3] David Figueroa,[3] Douglas MacNeil,[1] Margaret A. Cascieri,[1] Ravi Nargund,[2] Raman Bakshi,[2] Mark Abramovitz,[4] Rino Stocco,[4] Stacia Kargman,[4] Gary O'Neill,[4] Lex H. T. Van Der Ploeg,[1] Jilly Evans,[4] Arthur A. Patchett,[2] Roy G. Smith,[5] Andrew D. Howard[1]†

Motilin is a 22–amino acid peptide hormone expressed throughout the gastrointestinal (GI) tract of humans and other species. It affects gastric motility by stimulating interdigestive antrum and duodenal contractions. A heterotrimeric guanosine triphosphate–binding protein (G protein)–coupled receptor for motilin was isolated from human stomach, and its amino acid sequence was found to be 52 percent identical to the human receptor for growth hormone secretagogues. The macrolide antibiotic erythromycin also interacted with the cloned motilin receptor, providing a molecular basis for its effects on the human GI tract. The motilin receptor is expressed in enteric neurons of the human duodenum and colon. Development of motilin receptor agonists and antagonists may be useful in the treatment of multiple disorders of GI motility.

Gastrointestinal motility is a coordinated neuromuscular process that transports nutrients through the digestive system (*1*). Impaired GI motility, which can lead to gastroesophageal reflux disease, gastroparesis (diabetic and postsurgical), irritable bowel syndrome, and constipation, is one of the largest health care burdens of industrialized nations. Motilin, a peptide that is secreted by enterochromaffin cells of the small intestine (*2*), exerts a profound effect on gastric motility by inducing interdigestive (phase III) antrum and duodenal contractions (*3–5*). The structurally unrelated macrolide antibiotic erythromycin induces similar effects that are perhaps mediated by interaction with motilin receptors in the GI tract, accounting for erythromycin's side-effects, including vomiting, nausea, diarrhea, and abdominal muscular discomfort (*6, 7*).

Motilin is highly conserved across species and is synthesized as part of a larger inactive prohormone. Mature motilin (22 amino acids) is generated by removal of its secretory signal peptide and cleavage in its COOH-terminus (*8–11*). Although high-affinity binding sites for motilin have been detected in the GI tract of humans and other species and in the central nervous system of rabbits, their molecular structure has remained undefined (*12–18*). High-affinity (dissociation constant, $K_d \sim 2$ nM) and low-density (binding capacity, $B_{max} \sim$

[1]Department of Metabolic Disorders, [2]Department of Medicinal Chemistry, Merck Research Laboratories, Building RY-80Y-265, 126 East Lincoln Avenue, Rahway, NJ 07065, USA. [3]Department of Human Genetics, Merck Research Laboratories, Sumneytown Pike, West Point, PA 19486, USA. [4]Department of Biochemistry and Molecular Biology, Merck-Frosst Center for Therapeutic Research, 16711 TransCanada Highway, Kirkland, Quebec H9H 3L1, Canada. [5]Huffington Center on Aging and Department of Cell Biology, Baylor College of Medicine, One Baylor Plaza, Houston, TX 77030–3498, USA.

*These authors contributed equally to this work.
†To whom correspondence should be addressed. E-mail: howarda@merck.com